COMPREHENSIVE MODELING AND NUMERICAL SIMULATION OF INTERIOR BALLISTIC PROCESSES IN 120MM MORTAR WITH SYSTEMATIC EXPERIMENTAL VALIDATION

Ragini Acharya, Kenneth K. Kuo, Peter J. Ferrara
The Pennsylvania State University, University Park, PA, 16802

Henry T. Rand, Jr. and Joseph R. Nimphius
ARDEC, Picatinny Arsenal, NJ, 07806-5000

ABSTRACT

A three-dimensional mortar interior ballistic (3D-MIB) model and code have been developed and stage-wise validated with multiple sets of experimental data in close collaboration between The Pennsylvania State Univ. (PSU) and Army Research and Development Engineering Center. This newly developed MIB model and numerical code realistically simulates the combustion and pressurization processes in various components of the 120mm mortar system. Due to the complexity of the overall interior ballistic processes in the mortar propulsion system, the overall problem has been solved in a modular fashion, i.e., simulating each component of the mortar propulsion system separately. The physical processes in the mortar system are two-phase and were simulated by considering both phases as an interpenetrating continuum. Mass and energy fluxes from the flash tube into the granular bed of M1020 ignition cartridge were determined from a semi-empirical technique. For the tail-boom section, a transient one-dimensional two-phase numerical code based on method of characteristics (MOC) was developed and validated by experimental test results. The mortar tube combustion processes were modeled and solved by using a two-phase Roe-Pike method with van Leer flux limiter, a fourth order Runge-Kutta scheme, and an adaptive mesh generator to account for the projectile motion. For each component, the predicted pressure-time traces showed significant pressure wave phenomena, which closely simulated the measured pressure-time traces. The experimental data for the flash tube and ignition cartridge were obtained at PSU whereas the pressure-time traces at the breech-end of the mortar tube were obtained from the tests conducted at Yuma Proving Ground (YPG). The 3D-MIB code was also used to simulate the effect of flash tube vent-hole pattern on the pressure-wave phenomenon in the ignition cartridge. A comparison of the pressure difference between primer-end and projectile-end locations of the original and modified ignition cartridges with each other showed that the early-phase pressure-wave phenomenon can be significantly reduced with the modified pattern. The flow property distributions predicted by the 3D-MIB for a zero charge increment case are explained in details in this work.

INTRODUCTION

Simulation of the flame spreading and combustion processes in various parts of a 120mm mortar system under realistic firing conditions is important for design modification to improve the system performance. The motivation for this work came from critical safety failures of 120mm mortar ammunition which were investigated with the aid of detailed modeling and stepwise experimental validation of model predictions of the combustion behavior of the ignition cartridge and propelling charge increments in the mortar system. The 120mm mortar system consists of several major components including: 1) a percussion

Report Documentation Page

Form Approved
OMB No. 0704-0188

1. REPORT DATE **DEC 2008**	2. REPORT TYPE **N/A**	3. DATES COVERED **-**

4. TITLE AND SUBTITLE **Comprehensive Modeling And Numerical Simulation Of Interior Ballistic Processes In 120mm Mortar With Systematic Experimental Validation**	5a. CONTRACT NUMBER 5b. GRANT NUMBER 5c. PROGRAM ELEMENT NUMBER
6. AUTHOR(S)	5d. PROJECT NUMBER 5e. TASK NUMBER 5f. WORK UNIT NUMBER
7. PERFORMING ORGANIZATION NAME(S) AND ADDRESS(ES) **The Pennsylvania State University, University Park, PA, 16802**	8. PERFORMING ORGANIZATION REPORT NUMBER
9. SPONSORING/MONITORING AGENCY NAME(S) AND ADDRESS(ES)	10. SPONSOR/MONITOR’S ACRONYM(S) 11. SPONSOR/MONITOR’S REPORT NUMBER(S)

12. DISTRIBUTION/AVAILABILITY STATEMENT
Approved for public release, distribution unlimited

13. SUPPLEMENTARY NOTES
See also ADM002187. Proceedings of the Army Science Conference (26th) Held in Orlando, Florida on 1-4 December 2008, The original document contains color images.

14. ABSTRACT

15. SUBJECT TERMS

16. SECURITY CLASSIFICATION OF:			17. LIMITATION OF ABSTRACT	18. NUMBER OF PAGES	19a. NAME OF RESPONSIBLE PERSON
a. REPORT **unclassified**	b. ABSTRACT **unclassified**	c. THIS PAGE **unclassified**	**UU**	**8**	

primer to initiate the interior ballistic processes; 2) a flash tube with multiple vent holes to discharge combustion products of the pyrotechnic pellets; 3) a tail boom containing ignition cartridge loaded with M48 granular propellant for generating hot combustion products, rapid pressurization of the granular bed; 4) propellant charge increments containing M47 ball propellant mounted on the tail boom; 5) a projectile body containing explosives and a fuze system; and 6) a mortar tube that serves as a pressure vessel during the in-bore projectile acceleration. Due to the intricate design of the mortar system, the overall interior ballistic processes associated with mortar firings are extremely complicated. For realistic simulation of the physical and chemical processes in the mortar system, the 3D-MIB model and code were constructed in a modular fashion. The overall structure of the 3D-MIB code is shown in Fig. 1. This modular structure of the code also facilitates the independent execution of each of the subprograms, which were validated by distinct sets of experimental data. The major building blocks of the 3D-MIB model and code consist of:

a) Flash-tube sub-model: for simulating combustion behavior of igniter pellets and pressure wave phenomena in the flash tube;

b) Ignition cartridge sub-model: for simulating ignition delay, flame-spreading, pressurization, and discharge processes of gas and propellant particles from the tail-boom section;

c) Mortar tube combustion & projectile dynamics sub-model: for simulating ignition and combustion processes of the propelling charges and granular propellants from the tail-boom in a continuously expanding region in the mortar tube cavity as well as in-bore dynamics of the moving projectile.

Stage-wise validation of each sub-model was achieved by specially designed experimental setups. These include: 1) flash-tube igniter characterization test apparatus to determine the mass and energy fluxes at various vent-hole locations, 2) a windowed flash tube for *in situ* observation of the combustion behavior of igniter pellets and recording the pressurization process at various locations, 3) an instrumented stationary tail-boom section for studying the combustion and pressure-wave phenomena in the ignition cartridge loaded with granular propellants, 4) an instrumented mortar simulator (IMS) with multiple pressure transducer ports for recording the pressure-time traces at various locations. A series of tests was conducted by using each of the above carefully designed experimental test setups and first three sets of experiments were compared with the calculated results. The IMS test data could not be obtained currently at Aberdeen Test Center (ATC) due to scheduling conflicts, therefore; a set of experimental data from YPG was used to validate the numerical results for the mortar tube section.

IGNITION CARTRIDGE DATA AND COMBUSTION SUB-MODEL RESULTS

A transient two-phase model and numerical code using method of characteristics were developed and validated to simulate the interior ballistic processes of an ignition cartridge. From the experimental study, it was concluded that the physical processes in the ignition cartridge are independent of the azimuthal direction; therefore, a one-dimensional approach was suitable for this region. To simulate the combustion processes in the granular propellant bed loaded with M48 ball propellants, six coupled quasi-linear inhomogeneous hyperbolic partial differential equations were formulated by applying the principles of conservation of mass, momentum and energy for condensed and gas phases.

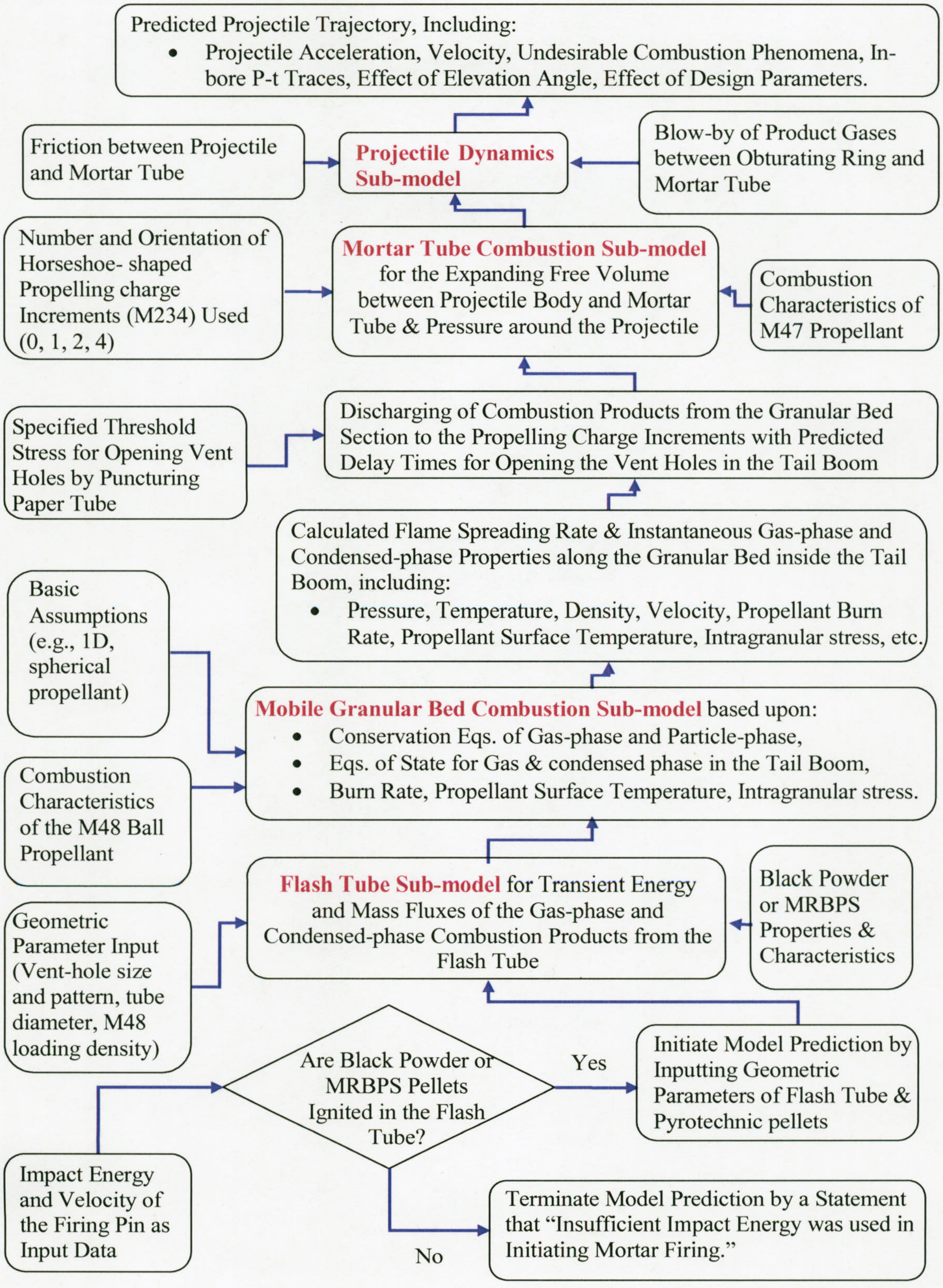

Figure 1. Overall Structure of the 3D Interior Ballistics Code

This system of equations was numerically solved for quantities of interest [i.e. pressure, propellant-surface temperature, gas temperature, porosity, gas velocity, and propellant particle velocity]; they were

converted to a system of ordinary differential equations using the method of characteristics. For hyperbolic equations, the flow properties at each point in the flow field depend on those properties in a finite region of the flow field in the domain of dependence, but are independent of the conditions in the future time. Thus marching-type numerical methods can be applied for obtaining the solutions of such flow fields. The detailed formulations and description of the solution procedure are given by Kuo et al.[1] The coupling of flash tube sub-model with the ignition cartridge sub-model was achieved by using the flash tube output of mass flow rates of discharged gas and condensed-phase products as well as their corresponding energy fluxes from the flash-tube vent holes to the granular propellant bed. A good agreement between the predicted and experimental results was demonstrated as shown by the Acharya and Kuo.[2,3] These sub-models were also used to estimate the effect of two different igniter materials (Black powder and MRBPS), which were validated with the experimental data obtained at PSU.[4] In this work, the effect of vent-hole patterns on the interior ballistic processes in the ignition cartridge was numerically simulated. A comparison of original (baseline) and modified flash tube designs is presented here. The mass flow rate of gaseous products from the original flash tube into the granular bed at various axial locations is shown in Fig 2. The predicted pressure-time traces in the ignition cartridge at various axial locations are shown in Fig. 3. It can be seen from Fig. 3 that the pressure at Port 17 location (near projectile-end of granular bed) starts to rise before Port 0 location (near primer-end of granular bed). This behavior is attributed to stronger discharge of igniter products from the flash tube at $P_{4'}$ and $P_{5'}$ locations as shown in Fig. 2. It is useful to note that the predicted maximum pressure occurred in the axial location ($x' = 3.39$ cm) significantly below the P_1 transducer location, which was not measured in the earlier set of experiments. After the numerical results were known, a pressure transducer port called P_0 was added to the tail-boom section. The pressure-time traces with this modification exhibit a similar behavior to that of baseline flash tube in the ignition cartridge design.[4] In order to reduce the pressure-wave phenomenon in the ignition cartridge, the vent hole pattern on the flash tube was modified such that the vent holes close to the primer end are larger in diameter than those close to the projectile end. This modification increased the total vent-hole discharge area by about 22% in comparison with the original flash tube. The axial location of each vent hole did not change from that of original flash-tube design. The mass flow rate of gaseous products from the modified flash tube into the granular bed at various axial locations is shown in Fig 4. It is useful to note that the mass flow rate of hot gas-phase products discharging from different vent holes from the modified flash tube is much closer in their magnitudes than the original case. The predicted pressure-time traces at various axial locations in the ignition cartridge with modified flash tube are shown in Fig. 5. The pressure-time traces with this modification exhibit a similar behavior to that of the M1020 ignition cartridge with the original flash tube design. However, it can be observed that during the initial rise time, the differences in pressure at various port locations are much smaller than the case with the original flash tube. In the later period of the ballistic cycle, a pressure difference can still be observed, though its' magnitude is lower than that with the original flash-tube. A comparison of predicted pressure difference between the P_0 and P_{17} with experimental data is shown in Figs. 6(a)-6(b). The early-phase event is simulated closely by the model. The predicted results also simulate the effect of vent-hole modification on the granular bed pressurization processes as shown by absence of first peak in Fig. 6(b), which was duplicated by the experimental data.

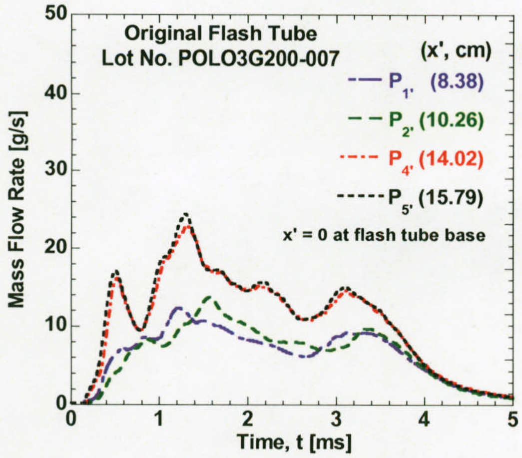

Figure 2. Calculated mass flow rate from original flash tube at various axial locations

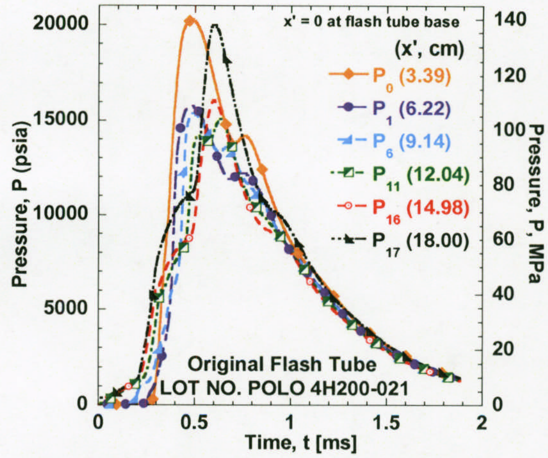

Figure 3. Calculated pressure-time traces in the ignition cartridge at various axial locations with original flash tube

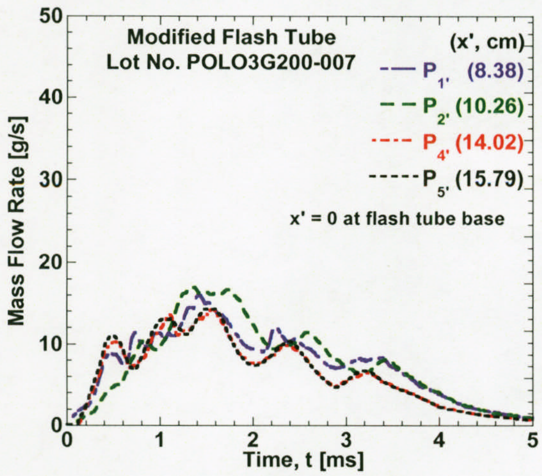

Figure 4. Calculated mass flow rate from modified flash tube at various axial locations

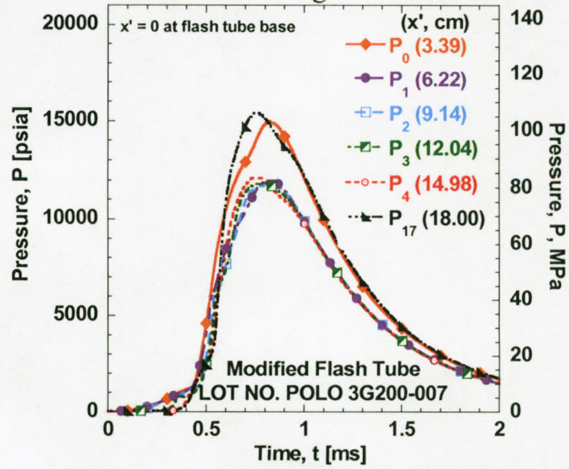

Figure 5. Calculated pressure-time traces in the ignition cartridge at various axial locations with modified flash tube

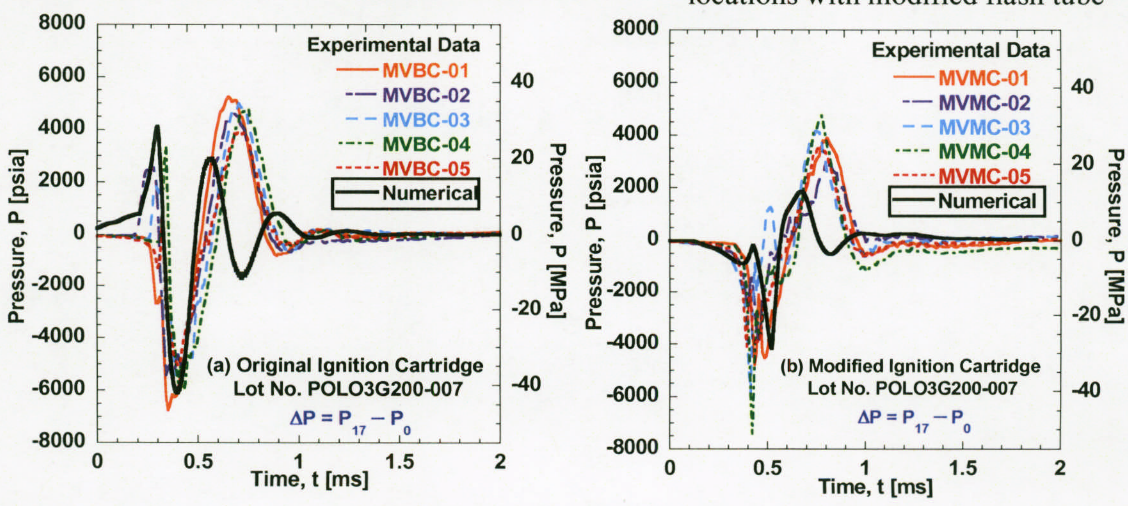

Figure 6.Comparisons of calculated and experimental pressure difference between primer-end and projectile-end locations on the original and modified ignition cartridges

MORTAR TUBE COMBUSTION & PROJECTILE DYNAMICS SUB-MODEL

The two-phase transient gas dynamic behavior of hot products gases and particles from the vent holes of the tail-boom section are coupled with the heat-transfer, flame-spreading, combustion, and chamber pressurization processes in the mortar tube. In the mortar tube sub-model, these data are used in the boundary conditions and as source terms in the governing equations as shown in Eqs. (1) and (2):

$$\frac{\partial(\rho\phi V)}{\partial t}+\frac{\partial(\phi\rho U_{g,z}V)}{\partial z}+\frac{1}{r}\frac{\partial(r\phi\rho U_{g,r}V)}{\partial r}+\frac{1}{r}\frac{\partial(\phi\rho U_{g,\theta}V)}{\partial\theta}$$
$$= A_{sb}\rho_p r_b + \underbrace{\alpha_g}_{\substack{=1 \text{ if a TB vent}\\ \text{hole is there,}\\ =0 \text{ otherwise}}} \times \underbrace{\dot{m}_{TBvhg}}_{\substack{\text{Gas-phase mass}\\ \text{added from tail-}\\ \text{boom region}}} + \alpha_g \times \underbrace{(\dot{m}_b)_{TB,Ej}}_{\substack{\text{Gaseous mass added}\\ \text{from continued}\\ \text{combustion of ejected}\\ \text{particles from tail-boom}}} \quad (1)$$

$$\frac{\partial(\phi^c\rho_p V)}{\partial t}+\frac{\partial(\phi^c\rho_p U_{p,z}V)}{\partial z}+\frac{\partial(r\phi^c\rho_p U_{p,r}V)}{r\partial r}+\frac{\partial(\phi^c\rho_p U_{p,\theta}V)}{r\partial\theta}$$
$$= -A_{sb}\rho_p r_b V + \underbrace{\alpha_p}_{\substack{=1 \text{ if a TB vent}\\ \text{hole is there,}\\ =0 \text{ otherwise}}} \times \underbrace{\dot{m}_{TBvhc}}_{\substack{\text{Particle mass}\\ \text{added from TB}}} - \alpha_p \times \underbrace{(\dot{m}_b)_{TB,Ej}}_{\substack{\text{Particle mass loss}\\ \text{from continued}\\ \text{combustion of ejected}\\ \text{particles from TB}}} \quad (2)$$

where, $\phi^c \equiv 1-\phi$ and V is the local volume.

In the above equations, subscript TB-Ej means ejected mass from the tail boom (TB). The number of particles ejected from the tail-boom vent holes is determined by the mass discharge rate of condensed-phase material. Due to the complex projectile geometry, an unstructured mesh was used to discretize the computational domain as shown in Fig. 7. As the projectile starts moving, a dynamic mesh generation scheme was used to continuously discretize the new space in the breech area. This mesh is also a combination of hexahedral/tetrahedral elements. For solving the six coupled PDEs, a Roe-Pike average solver with entropy fix was used. A van Leer flux limiter was utilized to improve the solution at the contact discontinuities and shock fronts. The fourth-order Runge-Kutta method was used for integration of the source terms in the governing equations. Prior to using this numerical scheme for mortar tube, the solution was verified using an exact solution for the Riemann shock tube problem. Thereafter, predicted results were obtained for the mortar tube with 0 charge increments and results are validated with the experimental data for breech pressure from YPG. The non-uniform axial variation of the discharging combustion products from tail-boom causes the sequential pressurization event in the mortar tube. The pressure-waves are generated and they propagate in both directions toward fin-blade region and projectile-payload region. These waves subside with the projectile motion as shown in *x-t* diagrams for pressure, axial gas velocity, particle velocities, and porosity in Figs. 8(a)-(e). The *x-t* diagrams for porosity and particle velocity show the initial downward motion of propellant grains towards breech and later movement towards the projectile driven by the gas motion. The *x-t* diagram for early-phase pressure variations are shown in Fig. 8(b), which demonstrates strong compression and rarefaction waves in the mortar tube. The comparison of calculated breech pressure-time trace with the experimental data shows excellent agreement in Fig. 9. The predicted projectile trajectory and velocity are shown in Fig. 10.

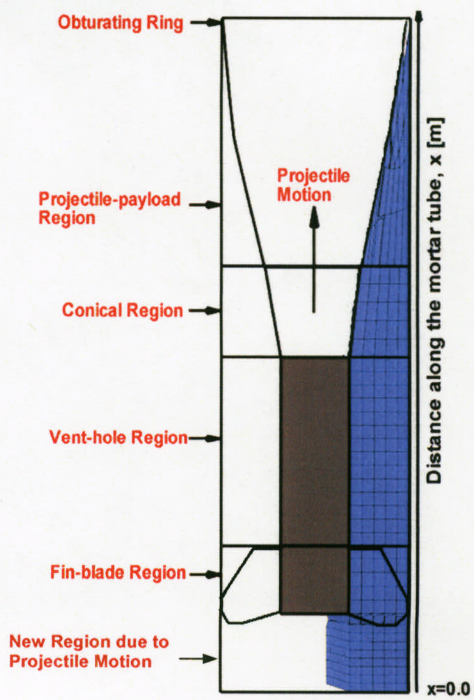

Figure 7. Description of mortar tube mesh and various regions

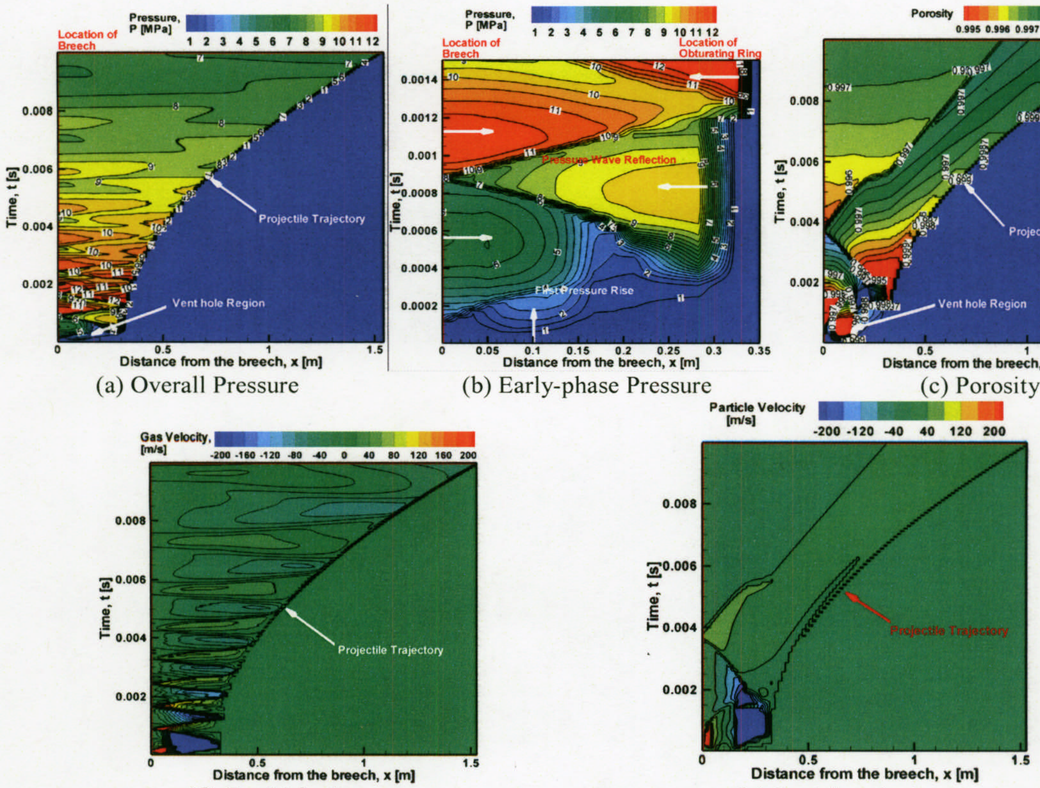

(a) Overall Pressure (b) Early-phase Pressure (c) Porosity

(d) Gas Velocity (e) Particle velocity

Figure 8. The *x-t* diagram in the mortar tube section with moving projectile

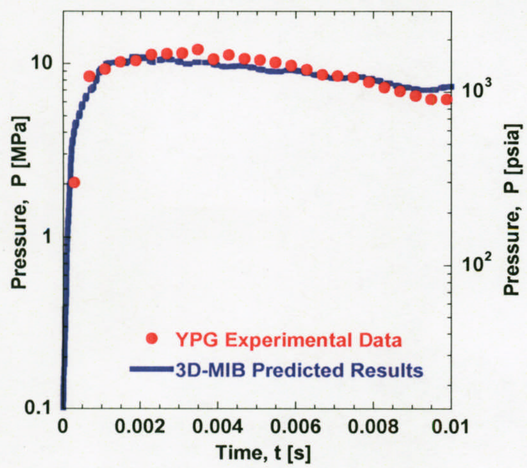

Figure 9. Comparison of measured breech pressure with the computed results

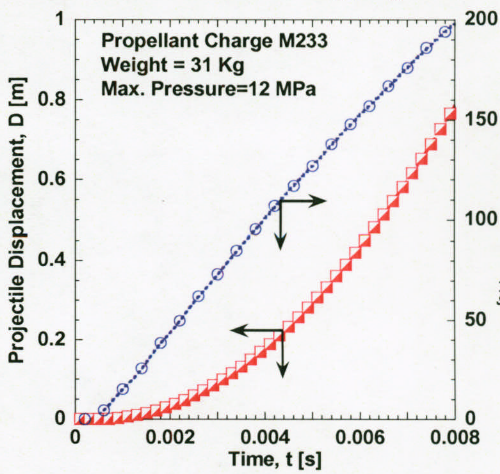

Figure 10. Predicted projectile trajectory and projectile velocity results

CONCLUSIONS

This paper demonstrated usefulness of the 3D-MIB comprehensive model and efficient numerical code in the prediction of interior ballistic processes in the 120mm mortar system. The model and code can also be applied to different sized mortar systems. Furthermore, this code has capability to simulate the interior ballistics of small and medium-caliber gun systems. Overall, the 3D-MIB code should be an extremely useful tool for advancing the state-of-the-art for both mortar and gun systems. Therefore, it can greatly benefit the future combat systems of the US Army.

The overall 3D-MIB code has been designed to have many independent subprograms for each physical component of the mortar system. Each subprogram was validated by specially designed experiments. This approach is effective since some subsystems can be tested and simulated easily. The modular design of 3D-MIB code enables the users to apply the code without any major modification when one or more physical components are upgraded or changed in their design. Stable and efficient numerical techniques have been adopted, which permit the code to be executed on a personal computer or single processor or a multiple processor machine with shared memory. The 3D-MIB code can also be used to provide the guidance for design and performance improvements of the mortar projectile.

- Effect of different primer material, flash tube geometry, pellet configurations, granular bed loading densities, vent-hole distributions can be studied as demonstrated by this work.
- The numerical code can be helpful to acquire deeper understanding of the ballistic processes of mortar systems.
- 3D-MIB code can provide predicted pressure-time traces and many other physical parameter variations at multiple axial locations. These physical parameter variations are useful for reducing the pressure wave phenomena during the interior ballistic cycle in the mortar firing.
- The knowledge gained from the simulation of these processes can help to reduce the possibilities for critical failures during operation in the field by better understanding the combustion process and the resulting peak pressures and pressure waves.
- The 3D-MIB code can also be used as an analytical tool for studying any abnormal behavior of the mortar projectile during operation. For example, the local region overpressure generated by aligning all charge increments in one orientation or the effect of out of spec flash tube vent holes.
- The numerical simulation with the code can be used to replace or reduce the need for expensive ballistic test firing throughout the lifecycle of the program.

ACKNOWLEDGMENT

The authors would like to acknowledge the support from US Army through contract no. DAAE30-03-D-1008, managed by Mr. Jack Sacco of Savit Corporation.

REFERENCES

1. K. K. Kuo, R. Acharya, P.J. Ferrara, and J. D. Moore, "Method of Characteristics Simulation of Interior Ballistic Processes of M1020 Ignition Cartridge in a 120mm Mortar System," *Advancements in Energetic Materials & Chemical Propulsion*, Vol. 1, 2007, pp. 621-642.
2. R. Acharya and K. K. Kuo, "Finite Element Simulation of Interior Ballistic Processes in 120mm Mortar Systems," *Proceedings of International Symposium on Ballistics*, Vol. 1, 2007, pp. 343-350.
3. R. Acharya and K. K. Kuo, "Effect of Different Flash-tube Vent-hole Patterns on Interior Ballistic Processes of Ignition Cartridge of 120mm Mortar System," accepted for publication in *Energetic Material Synthesis and Combustion Characterization for Chemical Propulsion*, 2008.
4. J.D.Moore, K.K.Kuo, R. Acharya, and P.J.Ferrara, "Effect of Flash-tube Vent-hole Patterns on the Combustion Product Discharge Rate", accepted for publication in *Energetic Material Synthesis and Combustion Characterization for Chemical Propulsion*, 2008.
5. E. F. Toro, Riemann Solvers and Numerical Methods for Fluid Dynamics, 2nd Edition, Springer-Verlag Pubs., 1999.
6. R. J. LeVeque, Numerical Methods for Conservation Laws, Lectures in Mathematics, Birkhäuser, 1990.